

# Analytical Methods

Accepted Manuscript



This is an *Accepted Manuscript*, which has been through the Royal Society of Chemistry peer review process and has been accepted for publication.

*Accepted Manuscripts* are published online shortly after acceptance, before technical editing, formatting and proof reading. Using this free service, authors can make their results available to the community, in citable form, before we publish the edited article. We will replace this *Accepted Manuscript* with the edited and formatted *Advance Article* as soon as it is available.

You can find more information about *Accepted Manuscripts* in the [Information for Authors](#).

Please note that technical editing may introduce minor changes to the text and/or graphics, which may alter content. The journal's standard [Terms & Conditions](#) and the [Ethical guidelines](#) still apply. In no event shall the Royal Society of Chemistry be held responsible for any errors or omissions in this *Accepted Manuscript* or any consequences arising from the use of any information it contains.

1  
2  
3  
4  
5  
6  
7  
8  
9  
10  
11 **Application of silver nanoparticles decorated with**  
12  **$\beta$ -cyclodextrin in determination of 6-mercaptopurine**  
13 **by Surface-enhanced Raman Spectroscopy**  
14  
15  
16  
17  
18  
19  
20  
21  
22  
23  
24  
25

26 Lei Yang, Yanhua Chen, Hongli Li, Lan Luo, Ying Zhao, Hanqi Zhang, Yuan Tian \*  
27

28 *College of Chemistry, Jilin University, Changchun, 130012, P. R. China*  
29  
30  
31  
32  
33  
34  
35  
36  
37  
38  
39  
40

41 *\*To whom correspondence should be addressed.*  
42

43 *Phone: +86-431-85168399;*  
44

45 *Fax: +86-431-85112355*  
46  
47

48 *E-mail: tianyuan@jlu.edu.cn*  
49  
50  
51  
52  
53  
54  
55  
56  
57  
58  
59  
60

## Abstract

Although classical silver nanospheres were widely used as the probes in surface-enhanced Raman spectroscopy (SERS), they lacked long-term stability. In the present work, the silver nanoparticles decorated with  $\beta$ -cyclodextrin ( $\beta$ -CD-AgNPs) were used as the probe and the stability was improved. The adsorption characteristics of 6-mercaptopurine (6-MP) on classical silver nanospheres and  $\beta$ -CD-AgNPs were studied cautiously using SERS, and chemical information of the molecular structure was obtained. The binding of 6-MP molecule to the surface of AgNPs is based on the stable Ag-S covalent bond. The electrostatic adsorption between protonated N<sup>7</sup> atom or N<sup>1</sup> atom and the silver surface results in a notable Raman enhancement. The intensity of the Raman band of 6-MP at 866 cm<sup>-1</sup> was used to determine 6-MP. The experimental conditions, such as volume of CD-AgNPs solution, incubation time, pH value and concentration of sodium chloride were examined and optimized. Compared with classical silver nanospheres when  $\beta$ -CD-Ag nanoparticles were used, the sensitivity was higher, the analytical time was shorter, and the linear range was wider. A good linearity ( $r=0.996$ ) in the range of  $(0.040-2.0) \times 10^{-7} \text{ mol}\cdot\text{L}^{-1}$  was obtained for determining 6-MP. The limit of detection is  $0.024 \times 10^{-7} \text{ mol}\cdot\text{L}^{-1}$  and the limit of quantification is  $0.080 \times 10^{-7} \text{ mol}\cdot\text{L}^{-1}$ . This method was successfully applied to the

determination of 6-MP in real samples and the results were satisfactory.

*Keywords:*  $\beta$ -cyclodextrin ( $\beta$ -CD); Silver nanoparticles (AgNPs);  
6-mercaptopurine (6-MP); Surface-enhanced Raman spectroscopy  
(SERS)

## 1. Introduction

Surface-enhanced Raman spectroscopy (SERS) technique demonstrates unique advantages in material analysis and enjoys a huge potential as a high sensitive method of quantitative analysis. First of all, because of obvious and tangible molecular specificity, SERS is an extremely convenient method to get content information of the analyte in the sample and the structure information of the molecule simultaneously. The SERS can be applied to the simultaneous detection of multiple analytes because all molecules own their own characteristic Raman signals<sup>1-3</sup>. Secondly, SERS is superior to other methods in providing information of the surface properties, because its real-time signal will change with many factors such as the chemical environment (such as pH value) and the orientation or rearrangement of molecules adsorbed on the substrate surface<sup>4-5</sup>.

Among a great variety of available SERS substrates, multifarious silver colloids are often used due to high activity and strong operability<sup>6-12</sup>. Silver colloids generally used for SERS active substrate were prepared by reducing silver nitrate with hydrazine, sodium borohydride<sup>13</sup> or sodium citrate<sup>14</sup>. The dispersion and stability of the silver colloids were achieved based on electrostatic repulsion between the nanoparticles.

1  
2  
3  
4 However, there are numerous external irresistible factors that will lead  
5  
6 the repulsive force somewhat to be weakened or even to disappear, so  
7  
8 that silver nanoparticles in the solution are no longer stable and then  
9  
10 coagulate. The uncontrolled coagulation eventually lead to a sharp  
11  
12 decrease of the activity of SERS substrate and poor stability in the form  
13  
14 of SERS spectra. In conclusion, the preparation of silver nanoparticles  
15  
16 with excellent activity and stability is still difficult and a focus in current  
17  
18 research.  
19  
20  
21  
22

23  
24 Mercaptopurine (6-MP, Scheme 1) is a kind of chemotherapy drug  
25  
26 and can be used as immunosuppressor <sup>15</sup>. 6-MP is mainly used in the  
27  
28 treatment of lymphoblastic leukaemia, and used to treat variety of  
29  
30 diseases, such as choriocarcinoma, chorioadenoma, polycythemia,  
31  
32 psoriatic arthritis, and inflammatory bowel disease <sup>16</sup>. 6-MP dosage is an  
33  
34 issue of crucial importance and underdosage will fail in the treatment of  
35  
36 the disease. The relatively adverse effects can be caused by overdose. The  
37  
38 slight symptoms may be diarrhoea, nausea, vomiting, etc. while severe  
39  
40 symptoms can be hematuria, fatal liver toxicity, myelosuppression, etc.  
41  
42 <sup>17-18</sup>. Therefore, the determination of 6-MP is of great significance for  
43  
44 clinical applications. Some methods have been reported for the  
45  
46 determination of 6-MP, including HPLC <sup>19-21</sup>, GC/MS <sup>22</sup>, voltammetric  
47  
48 method <sup>23</sup>, electrochemical reductive desorption method <sup>24</sup>,  
49  
50 electrochemical method <sup>25</sup>, inhibition chemiluminescence <sup>26</sup>, flow  
51  
52  
53  
54  
55  
56  
57  
58  
59  
60

1  
2  
3  
4 injection chemiluminescence (FI-CL) <sup>27</sup>, and capillary electrophoresis  
5  
6 with laser-induced fluorescence detection <sup>28</sup> and fluorescence  
7  
8 enhancement detection <sup>29-30</sup>. However, these methods show their  
9  
10 limitations and demerits in practical application. The liquid  
11  
12 chromatography is time-consuming. GC/MS is not suitable to distinguish  
13  
14 between isomers. The electrochemical method requires frequently  
15  
16 calibration. To develop a simple and reliable method for determination of  
17  
18 6-MP is necessary.

19  
20  
21 In this work,  $\beta$ - cyclodextrin (  $\beta$ -CD ) was used as the protecting  
22  
23 agent to stabilize silver nanoparticles (AgNPs).  $\beta$ -CD modified AgNPs  
24  
25 were used as the substrate in SERS. 6-MP were covalently bonded on the  
26  
27 surface of the silver nanoparticles. The present method was applied to the  
28  
29 analysis of the real samples. The experimental results obtained using a  
30  
31 portable miniature Raman spectrometer indicated that the present method  
32  
33 had some advantages in sensitivity, simplicity, and rapidity.  
34  
35  
36  
37  
38  
39  
40  
41  
42

43  
44 *Scheme 1*  
45  
46  
47

## 48 49 **2. Experimental**

### 50 51 52 53 *2.1. Materials* 54 55 56 57 58 59 60

1  
2  
3 Silver nitrate ( $\text{AgNO}_3$ , 99.85 %), sodium citrate (anhydrous, 99 %),  
4  $\beta$ -cyclodextrin ( $\beta$ -CD, 98 %), ammonia ( $\text{NH}_3\cdot\text{H}_2\text{O}$ ), 6-mercaptopurine  
5  
6 (99.0 %), glucose, and sodium chloride ( $\text{NaCl}$ ) were purchased from  
7  
8 Beijing Ding Guo Biotech. Co. Ltd, China. The Britton-Robinson (BR)  
9  
10 buffer solution (ionic strength, 0.5) contained  $0.04 \text{ mol}\cdot\text{L}^{-1} \text{ H}_3\text{PO}_4$ ,  $0.04$   
11  
12  $\text{mol}\cdot\text{L}^{-1} \text{ HAc}$ , and  $0.04 \text{ mol}\cdot\text{L}^{-1} \text{ H}_3\text{BO}_3$  and the pH value of the buffer  
13  
14 solution was adjusted to appropriate pH using  $0.2 \text{ mol}\cdot\text{L}^{-1} \text{ NaOH}$ . BR  
15  
16 buffer solution was used to control the acidity of the system. Aqua regia  
17  
18 solution was used to clean the glassware and the glassware was then  
19  
20 rinsed thoroughly with deionized water prior to use. Other chemicals used  
21  
22 here were of analytical reagent grade and all the solutions used in this  
23  
24 study were prepared with deionized water obtained with Milli-Q water  
25  
26 purification system ( $18.2 \text{ M}\Omega\cdot\text{cm}$ ).  
27  
28  
29  
30  
31  
32  
33  
34  
35  
36  
37  
38

## 39 *2.2. Equipment*

40  
41  
42  
43 Raman spectra were obtained using a BTR111MiniRam (B&W Tek, Inc.),  
44  
45 equipped with 785 nm excitation laser and a fibre-optics probe. 1 cm  
46  
47 quartz cell was used. The laser power was chosen as 105 mW and the  
48  
49 integration time was 10s. Absorption spectra were recorded on an  
50  
51 Australian GBC Cintra 10e UV-vis-NIR spectrometer in the wavelength  
52  
53 range of 300 to 1000 nm. The TEM image was obtained with a  
54  
55  
56  
57  
58  
59  
60



1  
2  
3  
4 JEM-2100F transmission electron microscope operated at an accelerating  
5  
6 voltage of 200 kV.  
7  
8

### 9 10 11 *2.3.1. Synthesis of classical AgNPs* 12 13

14  
15 The AgNPs were synthesized based on the reduction of AgNO<sub>3</sub> by citrate  
16 following the procedure described by Lee and Meisel<sup>14</sup>. In a 250 mL  
17 round-bottom flask equipped with a condenser, 27 mg of AgNO<sub>3</sub> was  
18 dissolved in 150 mL of deionized water and heated to the boil with  
19 vigorous stirring. Rapid addition of 3 mL of 1 % sodium citrate in the  
20 boiling solution resulted in a green-gray and transparent colloid solution  
21 after boiling for 30 min. Then the heating was stopped and the stirring  
22 continued for an additional hour. Finally, the AgNPs were stored in a  
23 brown bottle at 4 °C  
24  
25  
26  
27  
28  
29  
30  
31  
32  
33  
34  
35  
36  
37  
38  
39  
40

### 41 *2.3.2. Synthesis of β-CD-AgNPs* 42 43 44

45 β-CD-AgNPs were prepared based on the traditional silver mirror  
46 reaction in the presence of cyclodextrin according to literature<sup>31</sup> except  
47 that α-CD was placed with β-CD, which resulted in significant change in  
48 the nanoparticles size. [Ag (NH<sub>3</sub>)<sub>2</sub>]<sup>+</sup> was prepared by adding ammonia  
49 dropwise into 1 mL of 0.1 mol·L<sup>-1</sup> AgNO<sub>3</sub> solution in a capped glass tube  
50  
51  
52  
53  
54  
55  
56  
57  
58  
59  
60

1  
2  
3  
4 and shaking vigorously till the precipitate was completely dissolved. The  
5  
6 mixture was diluted to 10 mL with deionized water to obtain the solution  
7  
8 of  $10 \text{ mmol}\cdot\text{L}^{-1} [\text{Ag}(\text{NH}_3)_2]^+$ . In a 250 mL round-bottom flask, 1.16 g of  
9  
10  $\beta$ -CD and 92 mL of deionized water were heated slightly for about 5 min  
11  
12 with vigorous stirring. Then 4 mL of  $10 \text{ mmol}\cdot\text{L}^{-1} [\text{Ag}(\text{NH}_3)_2]^+$  and 4  
13  
14 mL of  $50 \text{ mmol}\cdot\text{L}^{-1}$  glucose were added sequentially. The color of the  
15  
16 solution changed from colorless to light orange after boiling for 30 min  
17  
18 with refluxing and magnetic stirring. The resulting solution was cooled  
19  
20 down to room temperature in atmospheric environment and filtered  
21  
22 through  $0.22 \mu\text{m}$  filter membrane. The solution could be stored for up to  
23  
24 45 days in refrigerator at  $4 \text{ }^\circ\text{C}$  without loss in activity.  
25  
26  
27  
28  
29  
30  
31  
32

#### 33 34 *2.4. Preparation of standard solution of 6-MP*

35  
36  
37

38  
39 The stock solution of  $3 \text{ mmol}\cdot\text{L}^{-1}$  6-MP was prepared by dissolving 6-MP  
40  
41 in a certain amount of  $0.1 \text{ mol}\cdot\text{L}^{-1}$  NaOH with the help of the ultrasound  
42  
43 and diluting to fixed volume with deionized water. The working standard  
44  
45 solution of 6-MP was prepared by diluting the stock solution with  
46  
47 deionized water. The resulting working standard solution was filtered  
48  
49 before use.  
50  
51  
52  
53  
54  
55

#### 56 57 *2.5. Preparation of sample*

58  
59  
60

1  
2  
3  
4  
5  
6 The commercial tablet was accurately weighed, ground, and transferred  
7 into a 50 mL flask. A certain amount of  $0.1 \text{ mol}\cdot\text{L}^{-1}$  NaOH solution was  
8 added in the flask and the flask was ultrasonically shaken for about 15  
9 min. The resulting solution was diluted to 250 mL with deionized water.  
10  
11  
12  
13  
14  
15  
16  
17  
18

### 19 *2.6. Determination of 6-MP*

20  
21  
22  
23 200  $\mu\text{L}$  of  $\beta\text{-CD-AgNPs}$  solution and 800  $\mu\text{L}$  of sample solution were  
24 added in the centrifuge tube and the resulting mixture was incubated for 2  
25 min. 100  $\mu\text{L}$  of buffer solution was added into the mixture. After gentle  
26 shaking, the appropriate volume of NaCl was added. The resulting  
27 solution was allowed to stand for 2 min at room temperature and then  
28 analyzed. The SERS intensity was expressed in the peak area. The peak  
29 area at  $866 \text{ cm}^{-1}$  was measured. All the experiments were performed in  
30 five replicates.  
31  
32  
33  
34  
35  
36  
37  
38  
39  
40  
41  
42

43 Similarly, 600  $\mu\text{L}$  AgNPs solution, 600  $\mu\text{L}$  of sample solution, 100  $\mu\text{L}$   
44 of buffer solution and appropriate volume of NaCl were mixed and the  
45 resulting solution was measured at  $866 \text{ cm}^{-1}$ .  
46  
47  
48  
49  
50  
51

## 52 **3. Results and discussion**

### 53 *3.1. Characterization of AgNPs and $\beta\text{-CD-AgNPs}$*

1  
2  
3  
4  
5  
6 UV-vis spectrum and TEM are routinely used to assess the dispersibility  
7 and morphology of noble metal nanoparticles. Fig. 1 shows the UV-vis  
8 spectrum and TEM image of the prepared silver nanoparticles. The  
9 absorption maximum of the AgNPs is at 420 nm with a full width at  
10 half-maximum (FWHM) of 115 nm. These values correspond to the  
11 monodisperse colloidal AgNPs with the diameter in the range of 50-60  
12 nm according to the literature <sup>11</sup>. The  $\beta$ -CD-AgNPs has a maximum  
13 absorption peak at 417 nm with FWHM of 71 nm. The size of the  
14  $\beta$ -CD-AgNPs was obtained by measuring 106 nanoparticles from their  
15 TEM images and the average diameter of the nanoparticles is 34.1 nm.  
16  
17  
18  
19  
20  
21  
22  
23  
24  
25  
26  
27  
28  
29  
30  
31  
32  
33  
34  
35  
36  
37  
38  
39  
40  
41  
42  
43  
44  
45  
46  
47  
48  
49  
50  
51  
52  
53  
54  
55  
56  
57  
58  
59  
60

The prepared  $\beta$ -CD-AgNPs are monodispersed and homogeneous.

The absorption spectra of  $\beta$ -CD-AgNPs in the presence and absence of 6-MP are given in Fig. 1. The  $\beta$ -CD-AgNPs in the absence of 6-MP exhibit an absorption peak at 400 nm. With the increase of NaCl concentration, the intensity of the surface plasmon absorption band decreases and the absorption peaks of  $\beta$ -CD-AgNPs are broadened. The experimental result indicates that the  $\beta$ -CD-AgNPs congregate in the solution. A new peak located at around 769 nm can be observed in the presence of 6-MP. 6-MP was bound to the surface of silver nanoparticles strongly, which caused the aggregation of silver nanoparticles and the enhancement of the SERS intensity. The absorption peak also reveals that

1  
2  
3  
4 the  $\beta$ -CD-AgNPs has a broad range of excitation wavelength and the laser  
5  
6 excitation wavelength of 785 nm is a reasonable choice.  
7  
8

9  
10  
11 **Figure 1**  
12

### 13 14 3.2. SERS bands of 6-MP 15 16 17

18  
19 Shen et al. have studied the SERS and orientation of 6-MP self-assembled  
20 monolayers (SAMs) on a silver electrode<sup>4</sup>. The Raman and SERS spectra  
21 of 6-MP on silver colloid were reported<sup>32</sup>, Fig. 2 shows the mechanism  
22 for determining 6-MP using  $\beta$ -CD-AgNPs as the SERS-active substrate.  
23  
24 The chemical force of CD to interact with AgNPs should be hydrogen  
25 bond between the  $\beta$ -CD rim hydroxyl groups and the noble metal  
26 particles, and the wider end of  $\beta$ -CD may sitting on the surface of AgNPs  
27  
28  
29 The chemical force of CD to interact with AgNPs should be hydrogen  
30 bond between the  $\beta$ -CD rim hydroxyl groups and the noble metal  
31 particles, and the wider end of  $\beta$ -CD may sitting on the surface of AgNPs  
32  
33  
34  
35  
36  
37  
38  
39  
40  
41  
42  
43  
44  
45  
46  
47  
48  
49  
50  
51  
52  
53  
54  
55  
56  
57  
58  
59  
60  
61  
62  
63  
64  
65  
66  
67  
68  
69  
70  
71  
72  
73  
74  
75  
76  
77  
78  
79  
80  
81  
82  
83  
84  
85  
86  
87  
88  
89  
90  
91  
92  
93  
94  
95  
96  
97  
98  
99  
100  
101  
102  
103  
104  
105  
106  
107  
108  
109  
110  
111  
112  
113  
114  
115  
116  
117  
118  
119  
120  
121  
122  
123  
124  
125  
126  
127  
128  
129  
130  
131  
132  
133  
134  
135  
136  
137  
138  
139  
140  
141  
142  
143  
144  
145  
146  
147  
148  
149  
150  
151  
152  
153  
154  
155  
156  
157  
158  
159  
160  
161  
162  
163  
164  
165  
166  
167  
168  
169  
170  
171  
172  
173  
174  
175  
176  
177  
178  
179  
180  
181  
182  
183  
184  
185  
186  
187  
188  
189  
190  
191  
192  
193  
194  
195  
196  
197  
198  
199  
200  
201  
202  
203  
204  
205  
206  
207  
208  
209  
210  
211  
212  
213  
214  
215  
216  
217  
218  
219  
220  
221  
222  
223  
224  
225  
226  
227  
228  
229  
230  
231  
232  
233  
234  
235  
236  
237  
238  
239  
240  
241  
242  
243  
244  
245  
246  
247  
248  
249  
250  
251  
252  
253  
254  
255  
256  
257  
258  
259  
260  
261  
262  
263  
264  
265  
266  
267  
268  
269  
270  
271  
272  
273  
274  
275  
276  
277  
278  
279  
280  
281  
282  
283  
284  
285  
286  
287  
288  
289  
290  
291  
292  
293  
294  
295  
296  
297  
298  
299  
300  
301  
302  
303  
304  
305  
306  
307  
308  
309  
310  
311  
312  
313  
314  
315  
316  
317  
318  
319  
320  
321  
322  
323  
324  
325  
326  
327  
328  
329  
330  
331  
332  
333  
334  
335  
336  
337  
338  
339  
340  
341  
342  
343  
344  
345  
346  
347  
348  
349  
350  
351  
352  
353  
354  
355  
356  
357  
358  
359  
360  
361  
362  
363  
364  
365  
366  
367  
368  
369  
370  
371  
372  
373  
374  
375  
376  
377  
378  
379  
380  
381  
382  
383  
384  
385  
386  
387  
388  
389  
390  
391  
392  
393  
394  
395  
396  
397  
398  
399  
400  
401  
402  
403  
404  
405  
406  
407  
408  
409  
410  
411  
412  
413  
414  
415  
416  
417  
418  
419  
420  
421  
422  
423  
424  
425  
426  
427  
428  
429  
430  
431  
432  
433  
434  
435  
436  
437  
438  
439  
440  
441  
442  
443  
444  
445  
446  
447  
448  
449  
450  
451  
452  
453  
454  
455  
456  
457  
458  
459  
460  
461  
462  
463  
464  
465  
466  
467  
468  
469  
470  
471  
472  
473  
474  
475  
476  
477  
478  
479  
480  
481  
482  
483  
484  
485  
486  
487  
488  
489  
490  
491  
492  
493  
494  
495  
496  
497  
498  
499  
500  
501  
502  
503  
504  
505  
506  
507  
508  
509  
510  
511  
512  
513  
514  
515  
516  
517  
518  
519  
520  
521  
522  
523  
524  
525  
526  
527  
528  
529  
530  
531  
532  
533  
534  
535  
536  
537  
538  
539  
540  
541  
542  
543  
544  
545  
546  
547  
548  
549  
550  
551  
552  
553  
554  
555  
556  
557  
558  
559  
560  
561  
562  
563  
564  
565  
566  
567  
568  
569  
570  
571  
572  
573  
574  
575  
576  
577  
578  
579  
580  
581  
582  
583  
584  
585  
586  
587  
588  
589  
590  
591  
592  
593  
594  
595  
596  
597  
598  
599  
600  
601  
602  
603  
604  
605  
606  
607  
608  
609  
610  
611  
612  
613  
614  
615  
616  
617  
618  
619  
620  
621  
622  
623  
624  
625  
626  
627  
628  
629  
630  
631  
632  
633  
634  
635  
636  
637  
638  
639  
640  
641  
642  
643  
644  
645  
646  
647  
648  
649  
650  
651  
652  
653  
654  
655  
656  
657  
658  
659  
660  
661  
662  
663  
664  
665  
666  
667  
668  
669  
670  
671  
672  
673  
674  
675  
676  
677  
678  
679  
680  
681  
682  
683  
684  
685  
686  
687  
688  
689  
690  
691  
692  
693  
694  
695  
696  
697  
698  
699  
700  
701  
702  
703  
704  
705  
706  
707  
708  
709  
710  
711  
712  
713  
714  
715  
716  
717  
718  
719  
720  
721  
722  
723  
724  
725  
726  
727  
728  
729  
730  
731  
732  
733  
734  
735  
736  
737  
738  
739  
740  
741  
742  
743  
744  
745  
746  
747  
748  
749  
750  
751  
752  
753  
754  
755  
756  
757  
758  
759  
760  
761  
762  
763  
764  
765  
766  
767  
768  
769  
770  
771  
772  
773  
774  
775  
776  
777  
778  
779  
780  
781  
782  
783  
784  
785  
786  
787  
788  
789  
790  
791  
792  
793  
794  
795  
796  
797  
798  
799  
800  
801  
802  
803  
804  
805  
806  
807  
808  
809  
810  
811  
812  
813  
814  
815  
816  
817  
818  
819  
820  
821  
822  
823  
824  
825  
826  
827  
828  
829  
830  
831  
832  
833  
834  
835  
836  
837  
838  
839  
840  
841  
842  
843  
844  
845  
846  
847  
848  
849  
850  
851  
852  
853  
854  
855  
856  
857  
858  
859  
860  
861  
862  
863  
864  
865  
866  
867  
868  
869  
870  
871  
872  
873  
874  
875  
876  
877  
878  
879  
880  
881  
882  
883  
884  
885  
886  
887  
888  
889  
890  
891  
892  
893  
894  
895  
896  
897  
898  
899  
900  
901  
902  
903  
904  
905  
906  
907  
908  
909  
910  
911  
912  
913  
914  
915  
916  
917  
918  
919  
920  
921  
922  
923  
924  
925  
926  
927  
928  
929  
930  
931  
932  
933  
934  
935  
936  
937  
938  
939  
940  
941  
942  
943  
944  
945  
946  
947  
948  
949  
950  
951  
952  
953  
954  
955  
956  
957  
958  
959  
960  
961  
962  
963  
964  
965  
966  
967  
968  
969  
970  
971  
972  
973  
974  
975  
976  
977  
978  
979  
980  
981  
982  
983  
984  
985  
986  
987  
988  
989  
990  
991  
992  
993  
994  
995  
996  
997  
998  
999  
1000

Shen et al. have studied the SERS and orientation of 6-MP self-assembled monolayers (SAMs) on a silver electrode<sup>4</sup>. The Raman and SERS spectra of 6-MP on silver colloid were reported<sup>32</sup>, Fig. 2 shows the mechanism for determining 6-MP using  $\beta$ -CD-AgNPs as the SERS-active substrate. The chemical force of CD to interact with AgNPs should be hydrogen bond between the  $\beta$ -CD rim hydroxyl groups and the noble metal particles, and the wider end of  $\beta$ -CD may sitting on the surface of AgNPs<sup>33</sup>. The  $\beta$ -CD molecules have hydrophilic outer surface with hydroxyl groups, which can interact with AgNPs, and hydrophobic central cavity. 6-MP molecules can connect AgNPs with Ag-S bond when 6-MP in high concentration (6-MP molecules stand on the Ag surface); but maybe connect AgNPs with pi-Ag bond in low concentration (lie on the Ag surface). The  $\beta$ -CD can force 6-MP stand on the Ag surface either in high or low concentration.

As shown in Fig. 3, the dominating characteristic bands of the normal Raman and SERS spectra of 6-MP, ranging from 371 to 1499  $\text{cm}^{-1}$ , are

1  
2  
3  
4 all observed clearly. The difference of the spectra indicates that there is a  
5  
6 very strong interaction between 6-MP and  $\beta$ -CD-AgNPs. There are many  
7  
8 peaks in the SERS spectra of 6-MP. The major bands in these spectra are  
9  
10 located at 435, 623, 681, 866, 1003, 1145, 1207, 1288, and 1328  $\text{cm}^{-1}$ . Fig.  
11  
12 3a shows that all these bands are characteristic of 6-MP molecules  
13  
14 chemisorbed on the  $\beta$ -CD-AgNPs. The peak observed at 435  $\text{cm}^{-1}$   
15  
16 corresponds to  $\text{C}^6\text{-S}^{10}$  stretching vibration and ring breathing vibration.  
17  
18 The result suggests that 6MP should adsorb on the Ag surfaces through  
19  
20 the S atom. The strongest peak observed at 866  $\text{cm}^{-1}$  is mostly attributed  
21  
22 to the  $\text{C}^8\text{-H}^8$  out-of-plane bending vibration and  $\text{N}^7\text{-C}^8$  bending.  
23  
24 Subordinately, the peak observed at 1003  $\text{cm}^{-1}$  corresponds to  $\text{C}^4\text{-N}^9$   
25  
26 stretch, while the peak observed at 1145  $\text{cm}^{-1}$  is thought to come from  
27  
28  $\text{N}^7\text{-C}^8$  stretch,  $\text{C-N}^7\text{-H}^7$  bending, and  $\text{C}^5\text{-N}^7$  stretch. The overlapping peak  
29  
30 observed at 1288-1328  $\text{cm}^{-1}$  corresponds to the  $\text{C}^2\text{-H}^2$  and  $\text{C}^8\text{-H}^8$   
31  
32 deformation vibrations and the  $\text{N}^1\text{-C}^2\text{-N}^3$  stretching vibration. Therefore,  
33  
34 6-MP was adsorbed on the silver surface with a tilted orientation via S,  
35  
36  $\text{N}^1$ , and  $\text{N}^7$  atoms <sup>4</sup>. Weak peaks at 623, 681 and 1207  $\text{cm}^{-1}$  correspond to  
37  
38 ring  $\text{C}^5\text{-C}^6$  bending. An increase of SERS signal could be observed when  
39  
40 CD is decorated on AgNPs because of the change of surrounding  
41  
42 environment of AgNPs. The stability of AgNPs was improved in the  
43  
44 presence of  $\beta$ -CD.  
45  
46  
47  
48  
49  
50  
51  
52  
53  
54  
55  
56  
57  
58  
59  
60

**Figure 2**

*Figure 3*

### *3.4. Optimization of experimental conditions*

#### *3.4.1. Volume of $\beta$ -CD-AgNPs solution and incubation time*

The effect of the volume of  $\beta$ -CD-AgNPs solution in the range of 50  $\mu$ L to 400  $\mu$ L and the effect of incubation time on the SERS intensity were investigated. The experimental results are shown in Fig. 4. The results show the importance of properly controlling of the volume of  $\beta$ -CD-AgNPs and incubation time for obtaining an optimized Raman enhancement. For 50 and 100  $\mu$ L, the SERS intensities increase in the first 10 minutes. For 200  $\mu$ L, the SERS intensity reaches a clear-cut plateau in 2 min at room temperature and slightly changes after 8 min. For 300 and 400  $\mu$ L, the SERS intensities firstly increase and then decrease with the increase of incubation time. The SERS intensity increases with the increase of the amount of  $\beta$ -CD-AgNPs and go to a maximum at 300  $\mu$ L, and then the SERS intensity decreases with the increase of the amount of  $\beta$ -CD-AgNPs. 300  $\mu$ L should be the best choice. However, the accuracy of experimental results obtained with 300  $\mu$ L was lower than that obtained with 200  $\mu$ L. Therefore, 200 $\mu$ L and 2 min were

1  
2  
3  
4 selected in this method.

5  
6 For the AgNPs, as shown in Fig. 4, the reaction between silver  
7  
8  
9  
10  
11  
12  
13  
14  
15  
16  
17  
18  
19  
20  
21  
22  
23  
24  
25  
26  
27  
28  
29  
30  
31  
32  
33  
34  
35  
36  
37  
38  
39  
40  
41  
42  
43  
44  
45  
46  
47  
48  
49  
50  
51  
52  
53  
54  
55  
56  
57  
58  
59  
60  
For the AgNPs, as shown in Fig. 4, the reaction between silver nanospheres and 6-MP occurs rapidly and silver colloids can achieve the best coagulation at 4 min. After 4 min the SERS intensities decrease slightly. So, the incubation time 4 min was selected in this experiment.

*Figure 4*

#### 3.4.2. Effect of pH

29  
30  
31  
32  
33  
34  
35  
36  
37  
38  
39  
40  
41  
42  
43  
44  
45  
46  
47  
48  
49  
50  
51  
52  
53  
54  
55  
56  
57  
58  
59  
60  
The pH plays an important role in the experiment. BR buffer solution in the pH range of 2.7 to 6.7 was used to adjust the pH values of the analytical solution. Fig. 5 shows the effect of the pH value on the SERS intensity of the system. With the increase of pH value, the SERS intensity for the 6-MP increases, reaches maximum at pH 5.9, and then decreases significantly. So pH 5.9 of BR buffer solution was selected for the determination of 6-MP.

For the AgNPs, the silver colloids are negatively charged due to the adsorption of citrate groups, which is responsible for the stability of colloidal silver. It can be seen from Fig. 5 that the SERS intensity for the 6-MP reaches a maximum at the pH value of 3.5. When the pH value is higher than 3.5, there is a general trend of decreasing intensity. So pH 3.5



1  
2  
3  
4 was selected for the determination of 6-MP when AgNPs was used.  
5  
6  
7

8  
9 **Figure 5**  
10

11  
12  
13  
14 *3.4.3. Effect of concentration of sodium chloride*  
15  
16  
17

18  
19 An aggregating agent is routinely added into SERS-active colloids to  
20 achieve a degree of enhancement of SERS signals<sup>34</sup>. NaCl is frequently  
21 used as the aggregating agent for AgNPs in the enhancement process and  
22 the concentration of NaCl is an important factor for the aggregation  
23 degree of AgNPs<sup>31</sup>. The effect of sodium chloride concentration on the  
24 SERS intensity of 6-MP was investigated and the experimental results are  
25 shown in Fig. 6. The SERS intensity of 6-MP in the presence of  
26  $\beta$ -CD-AgNPs is enhanced gradually with the increase of NaCl  
27 concentration in the range of 0.12 mol·L<sup>-1</sup> to 0.31 mol·L<sup>-1</sup>. The peak area  
28 at 866 cm<sup>-1</sup> obtained with 0.22 mol·L<sup>-1</sup> NaCl solution is largest. Therefore,  
29 0.22 mol·L<sup>-1</sup> NaCl solution was selected for  $\beta$ -CD-AgNPs.  
30  
31  
32  
33  
34  
35  
36  
37  
38  
39  
40  
41  
42  
43  
44  
45

46 Similarly, 0.016 mol·L<sup>-1</sup> NaCl solution in the concentration range of  
47 0.012 mol·L<sup>-1</sup> to 0.020 mol·L<sup>-1</sup> was selected for AgNPs. The result  
48 indicates the Ag colloids have gotten to the optimum aggregation.  
49  
50  
51  
52  
53  
54

55  
56 **Figure 6**  
57  
58  
59  
60

### 3.5. Effect of coexisting substances

The coexisting substances with positive or negative charges will affect on the SERS intensity. The effect of the substances on the SERS intensity was investigated. The experimental results are summarized in Table 1. It can be seen that most of the foreign substances have little influence on the SERS intensity and can be allowed at high concentration levels. Compared with silver nanospheres, when the  $\beta$ -CD-AgNPs was used, selectivity was higher.

**Table 1**

### 3.6. Calibration curves and Stability of $\beta$ -CD-AgNPs

As shown in Fig. 7, the Raman peak at  $866\text{ cm}^{-1}$  is the strongest peak in the SERS spectra. Under the optimum conditions, the calibration curves were constructed by plotting the peak areas of the vibrational band at  $866\text{ cm}^{-1}$  versus the concentrations of analyte. For the  $\beta$ -CD-AgNPs, the SERS intensity is directly proportional to the 6-MP concentrations in the range of  $(0.040\text{-}2.0) \times 10^{-7}\text{ mol}\cdot\text{L}^{-1}$ . The regression equation is  $I_{\text{SERS}} = 108931 + 808173C$  ( $C$ :  $\text{mol}\cdot\text{L}^{-1}$ ). The correlation coefficient ( $r$ ) is 0.996 which indicates that there are good linear relationships between the SERS

intensity and 6-MP concentration. The limit of detection (LOD), corresponds to signal-to-noise ratio 3, is  $0.024 \times 10^{-7} \text{ mol} \cdot \text{L}^{-1}$ . The limit of quantification (LOQ) is  $0.080 \times 10^{-7} \text{ mol} \cdot \text{L}^{-1}$ . For the AgNPs, the regression equation is  $I_{\text{SERS}} = -335166 + 372791C$ . There is a linear relationship in the range of  $(0.80-4.8) \times 10^{-7} \text{ mol} \cdot \text{L}^{-1}$  and the corresponding correlation coefficient ( $r$ ) is 0.995. The LOD is  $0.14 \times 10^{-7} \text{ mol} \cdot \text{L}^{-1}$  and LOQ is  $0.47 \times 10^{-7} \text{ mol} \cdot \text{L}^{-1}$ . It can be concluded that compared with silver nanospheres, when  $\beta$ -CD-Ag were used the sensitivity for the determination of 6-MP was higher and the linear range was wider. Compared with methods reported previously, the SERS method using  $\beta$ -CD-AgNPs as substrates also has some advantages for 6-MP determination, as shown in Table 2. Fig. 8 shows that the  $\beta$ -CD-AgNPs as SERS substrates is stable within 45 days.

**Figure 7**

**Table 2**

**Figure 8**

### 3.7. Analytical application

The analytical applicability of the present method was validated by

1  
2  
3  
4 analyzing two commercial tablets of 6-MP. The results are shown in  
5  
6 Table 4. For the  $\beta$ -CD-AgNPs, the contents of the 6-MP per tablet in the  
7  
8 two samples are 51.5 and 51.0 mg. For the AgNPs, the contents of the  
9  
10 6-MP per tablet in the two samples are 43.0 and 38.2 mg, respectively.  
11  
12 Table 3 shows the recoveries and RSDs of 6-MP in the commercial tablet.  
13  
14 The results indicate that the two methods for determining 6-MP are  
15  
16 reliable and satisfactory. Compared with AgNPs, when the  $\beta$ -CD-AgNPs  
17  
18 were used, the recoveries are higher and RSD is lower.  
19  
20  
21  
22  
23  
24  
25  
26  
27  
28  
29  
30  
31  
32

**Table 3**

#### 33 **4. Conclusions**

34  
35  
36  
37 In this work, we report the preparation of  $\beta$ -CD-AgNPs nanoparticles and  
38  
39 describe a high sensitive and selective method for the determination of  
40  
41 6-MP. As the SERS substrate, the  $\beta$ -CD-AgNPs were more sensitive than  
42  
43 the AgNPs for determination 6-MP. The effects of some experimental  
44  
45 conditions are discussed and optimized in detail. A good linearity  
46  
47 ( $r=0.996$ ) in the range of  $(0.040-2.0) \times 10^{-7} \text{ mol}\cdot\text{L}^{-1}$  was obtained. In  
48  
49 addition, present method is suitable for the routine determination of 6-MP  
50  
51  
52  
53  
54  
55 in different dosage forms and also can be applied to drug control.  
56  
57  
58  
59  
60

**References:**

1. N. Guarrotxena and G. C. Bazan, *Advanced Materials*, 2014, 26, 1941-1946.
2. H. Kang, S. Jeong, Y. Park, J. Yim, B. H. Jun, S. Kyeong, J. K. Yang, G. Kim, S. Hong and L. P. Lee, *Advanced Functional Materials*, 2013, 23, 3719-3727.
3. C. L. Wong, U. Dinish, M. S. Schmidt and M. Olivo, *Analytica chimica acta*, 2014, 844, 54-60.
4. H. Chu, H. Yang, S. Huan, G. Shen and R. Yu, *The Journal of Physical Chemistry B*, 2006, 110, 5490-5497.
5. K. V. Kong, U. Dinish, W. K. O. Lau and M. Olivo, *Biosensors and Bioelectronics*, 2014, 54, 135-140.
6. R. A. Alvarez-Puebla and R. F. Aroca, *Analytical chemistry*, 2009, 81, 2280-2285.
7. L.-X. Chen, D.-W. Li, L.-L. Qu, Y.-T. Li and Y.-T. Long, *Analytical Methods*, 2013, 5, 6579-6582.
8. N. Leopold and B. Lendl, *The Journal of Physical Chemistry B*, 2003, 107, 5723-5727.
9. A. Raza and B. Saha, *Forensic science international*, 2014, 237, e42-e46.

10. J. Wu, F. Zhang and H. Zhang, *Carbohydrate polymers*, 2012, 90, 261-269.
11. Q. Yang, F. Liang, D. Wang, P. Ma, D. Gao, J. Han, Y. Li, A. Yu, D. Song and X. Wang, *Analytical Methods*, 2014, 6, 8388-8395.
12. J. P. Camden, J. A. Dieringer, Y. Wang, D. J. Masiello, L. D. Marks, G. C. Schatz and R. P. Van Duyne, *Journal of the American Chemical Society*, 2008, 130, 12616-12617.
13. R. Keir, D. Sadler and W. Smith, *Applied spectroscopy*, 2002, 56, 551-559.
14. P. Lee and D. Meisel, *The Journal of Physical Chemistry*, 1982, 86, 3391-3395.
15. S. Sahasranaman, D. Howard and S. Roy, *European journal of clinical pharmacology*, 2008, 64, 753-767.
16. O. Nielsen, B. Vainer and J. Rask - Madsen, *Alimentary pharmacology & therapeutics*, 2001, 15, 1699-1708.
17. B. Nørgård, L. Pedersen, K. Fonager, S. Rasmussen and H. T. Sørensen, *Alimentary pharmacology & therapeutics*, 2003, 17, 827-834.
18. A. R. Davis, L. Miller, H. Tamimi and A. Gown, *Obstetrics & Gynecology*, 1999, 93, 904-909.
19. T. L. Ding and L. Z. Benet, *Journal of Chromatography B: Biomedical Sciences and Applications*, 1979, 163, 281-288.

- 1  
2  
3  
4  
5  
6  
7  
8  
9  
10  
11  
12  
13  
14  
15  
16  
17  
18  
19  
20  
21  
22  
23  
24  
25  
26  
27  
28  
29  
30  
31  
32  
33  
34  
35  
36  
37  
38  
39  
40  
41  
42  
43  
44  
45  
46  
47  
48  
49  
50  
51  
52  
53  
54  
55  
56  
57  
58  
59  
60
20. Y. Su, Y. Y. Hon, Y. Chu, M. E. Van de Poll and M. V. Relling, *Journal of Chromatography B: Biomedical Sciences and Applications*, 1999, 732, 459-468.
  21. K. Tsutsumi, Y. Otsuki and T. Kinoshita, *Journal of Chromatography B: Biomedical Sciences and Applications*, 1982, 231, 393-399.
  22. S. Floberg, P. Hartvig, B. Lindström, G. Lönnnerholm and B. Odling, *Journal of Chromatography B: Biomedical Sciences and Applications*, 1981, 225, 73-81.
  23. M. Keyvanfard, V. Khosravi, H. Karimi-Maleh, K. Alizad and B. Rezaei, *Journal of Molecular Liquids*, 2013, 177, 182-189.
  24. Y. Sato, Y. Ishikawa, H. Matsuura, K. Uosaki, F. Mizutani and O. Niwa, *Electroanalysis*, 2005, 17, 965-968.
  25. P. Zhou, L. He, G. Gan, S. Ni, H. Li and W. Li, *Journal of Electroanalytical Chemistry*, 2012, 665, 63-69.
  26. H. Sun, T. Wang, X. Liu and P. Chen, *Journal of Luminescence*, 2013, 134, 154-159.
  27. L. Wang, B. Ling, H. Chen, A. Liang, B. Qian and J. Fu, *Luminescence*, 2010, 25, 431-435.
  28. S. R. Rabel, J. F. Stobaugh and R. Trueworthy, *Analytical biochemistry*, 1995, 224, 315-322.
  29. X.-C. Shen, L.-F. Jiang, H. Liang, X. Lu, L.-J. Zhang and X.-Y. Liu,

- 1  
2  
3  
4  
5  
6  
7  
8  
9  
10  
11  
12  
13  
14  
15  
16  
17  
18  
19  
20  
21  
22  
23  
24  
25  
26  
27  
28  
29  
30  
31  
32  
33  
34  
35  
36  
37  
38  
39  
40  
41  
42  
43  
44  
45  
46  
47  
48  
49  
50  
51  
52  
53  
54  
55  
56  
57  
58  
59  
60
- Talanta*, 2006, 69, 456-462.
30. Z. Chen, G. Zhang, X. Chen, J. Chen, J. Liu and H. Yuan,  
*Biosensors and Bioelectronics*, 2013, 41, 844-847.
31. P. Ma, F. Liang, Y. Sun, Y. Jin, Y. Chen, X. Wang, H. Zhang, D.  
Gao and D. Song, *Microchimica Acta*, 2013, 180, 1173-1180.
32. A. V. Szeghalmi, L. Leopold, S. Pînzaru, V. Chis, I.  
Silaghi-Dumitrescu, M. Schmitt, J. Popp and W. Kiefer, *Journal of  
Molecular Structure*, 2005, 735-736, 103-113.
33. S. Jaiswal, B. Duffy, A. K. Jaiswal, N. Stobie and P. McHale,  
*International journal of antimicrobial agents*, 2010, 36, 280-283.
34. N. R. Yaffe, A. Ingram, D. Graham and E. W. Blanch, *Journal of  
Raman Spectroscopy*, 2009, 41, 618-623.



1  
2  
3  
4  
5  
6  
7  
8  
9  
10  
11  
12  
13  
14  
15  
16  
17  
18  
19  
20  
21  
22  
23  
24  
25  
26  
27  
28  
29  
30  
31  
32  
33  
34  
35  
36  
37  
38  
39  
40  
41  
42  
43  
44  
45  
46  
47  
48  
49  
50  
51  
52  
53  
54  
55  
56  
57  
58  
59  
60

Figure Captions:

Scheme 1: Structure of 6-Mercaptopurine in thiol form (a) and its tautomer (b).

Fig. 1: (A) UV-Vis spectrum of AgNPs (a),  $\beta$ -CD-AgNPs (b),  $\beta$ -CD-AgNPs in the presence of NaCl ( $0.22 \text{ mol}\cdot\text{L}^{-1}$ ) and trace 6-MP (c) and  $\beta$ -CD-AgNPs in the presence of NaCl ( $0.22 \text{ mol}\cdot\text{L}^{-1}$ ) (d). (B) Statistical analysis of the size distribution of  $\beta$ -CD-AgNPs. (C) The TEM image of  $\beta$ -CD-AgNPs. (D) The TEM image of  $\beta$ -CD-AgNPs in the presence of NaCl ( $0.22 \text{ mol}\cdot\text{L}^{-1}$ )

Fig. 2: The sensing mechanism for determining 6-MP using  $\beta$ -CD-AgNPs as the SERS-active substrate

Fig. 3: Raman and SERS spectra of 6-MP. SERS spectrum of 6-MP based on  $\beta$ -CD-AgNPs, the concentration of 6-MP is  $1.0\times 10^{-7} \text{ mol}\cdot\text{L}^{-1}$  (a), SERS spectrum of 6-MP based on AgNPs, the concentration of 6-MP is  $1.0\times 10^{-7} \text{ mol}\cdot\text{L}^{-1}$  (b), Raman spectrum of solid 6-MP (c), Raman spectrum of 6-MP ( $10 \text{ mmol}\cdot\text{L}^{-1}$ ) (d). 785 nm laser wavelength, 10 s exposure time, 150 mW laser power.

Fig. 4: Effects of volume of  $\beta$ -CD-AgNPs solution and incubation time on SERS intensity of 6-MP. For  $\beta$ -CD-AgNPs, the concentration of 6-MP is  $1.0\times 10^{-7} \text{ mol}\cdot\text{L}^{-1}$ , the concentration of

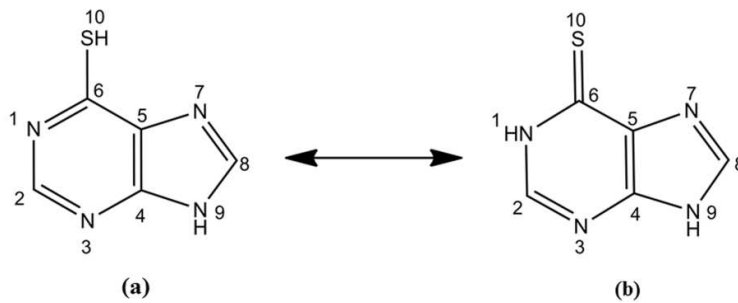
NaCl is  $0.22 \text{ mol}\cdot\text{L}^{-1}$ , pH is 5.9. For AgNPs, the concentration of 6-MP is  $2.4\times 10^{-7} \text{ mol}\cdot\text{L}^{-1}$ , the concentration of NaCl is  $0.016 \text{ mol}\cdot\text{L}^{-1}$ , pH is 3.5.

Fig. 5: Effect of pH on SERS intensity of 6-MP. For AgNPs, the concentration of 6-MP is  $2.4\times 10^{-7} \text{ mol}\cdot\text{L}^{-1}$ , the concentration of NaCl is  $0.016 \text{ mol}\cdot\text{L}^{-1}$  (a). For  $\beta$ -CD-AgNPs, the concentration of 6-MP is  $1.0\times 10^{-7} \text{ mol}\cdot\text{L}^{-1}$ , the concentration of NaCl is  $0.22 \text{ mol}\cdot\text{L}^{-1}$  (b).

Fig. 6: Effect of concentration of NaCl on SERS intensity of 6-MP. For AgNPs, the concentration of 6-MP is  $2.4\times 10^{-7} \text{ mol}\cdot\text{L}^{-1}$ , pH is 3.5 (a). For  $\beta$ -CD-AgNPs, the concentration of 6-MP is  $1.0\times 10^{-7} \text{ mol}\cdot\text{L}^{-1}$ , pH is 5.9 (b).

Fig. 7: Calibration curves of 6-MP and photographic images of  $\beta$ -CD-AgNPs and AgNPs. Error bars represent the standard deviation of five measurements. For  $\beta$ -CD-AgNPs, the concentration of NaCl is  $0.22 \text{ mol}\cdot\text{L}^{-1}$ , pH is 5.9. For AgNPs, the concentration of NaCl is  $0.016 \text{ mol}\cdot\text{L}^{-1}$ , pH is 3.5.

Fig. 8: Effects of storage time of  $\beta$ -CD-AgNPs at  $4 \text{ }^\circ\text{C}$  on SERS intensity of 6-MP, Inset shows the SERS intensity distribution of the  $866\text{cm}^{-1}$  band. Each datum point represents the average value of the experimental results obtained in five replicates. Error bar represents the standard deviation.



Scheme 1

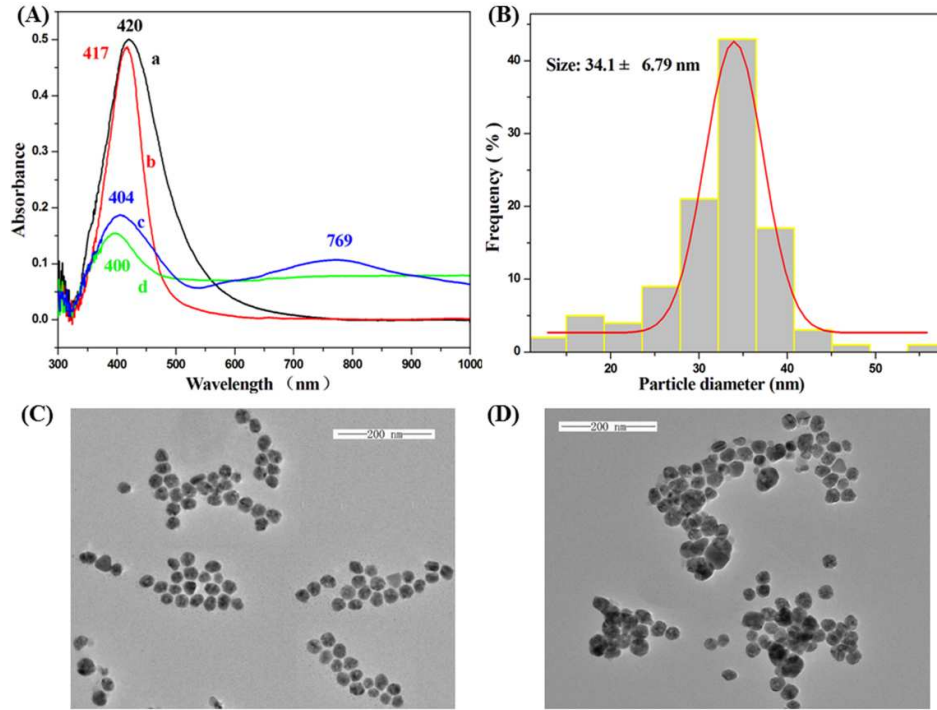


Fig. 1

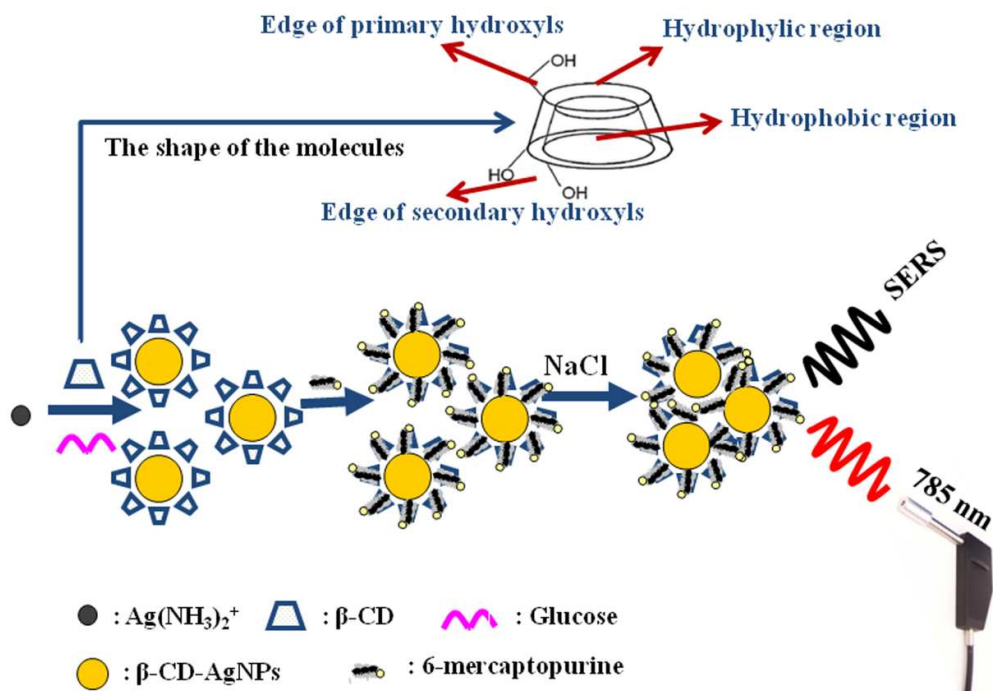


Fig. 2

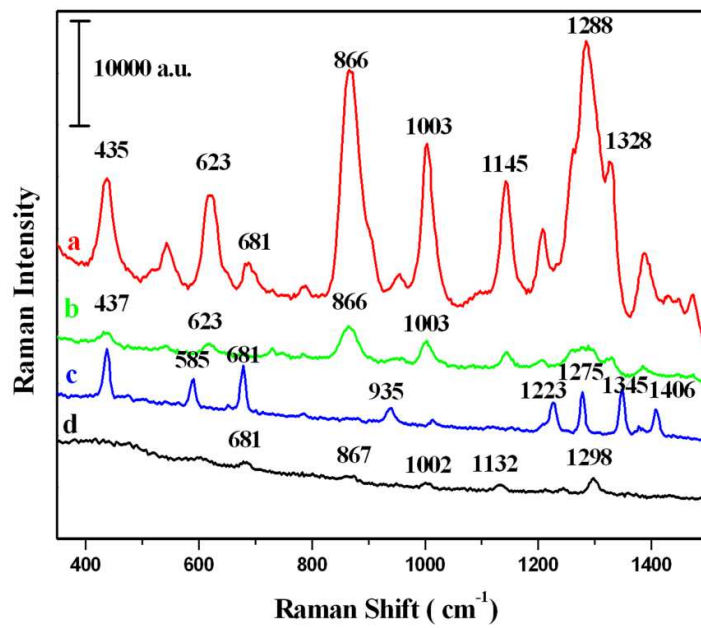


Fig. 3

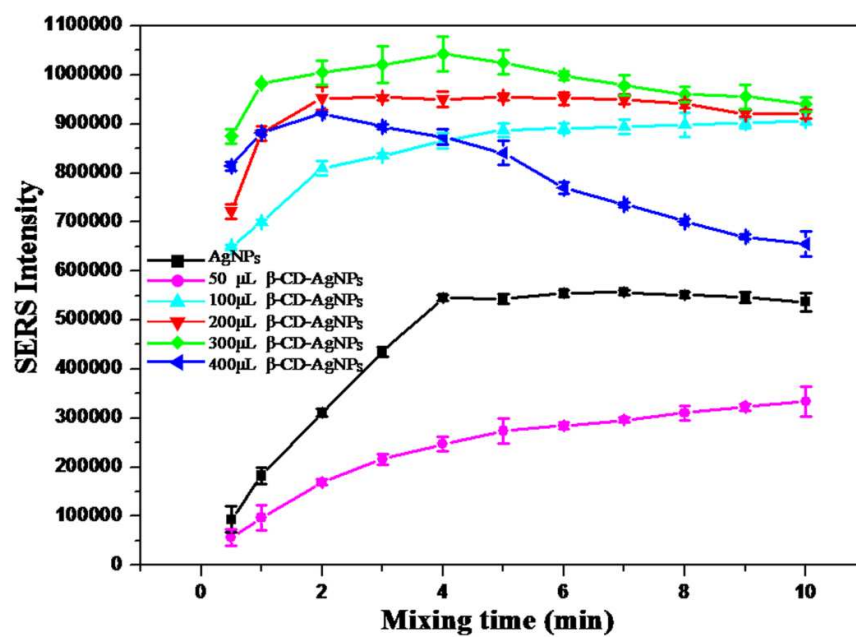


Fig. 4

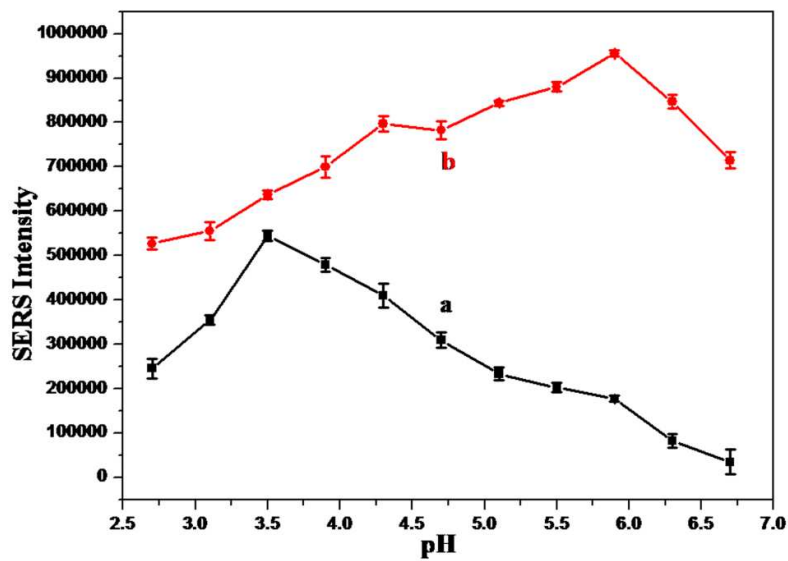


Fig. 5



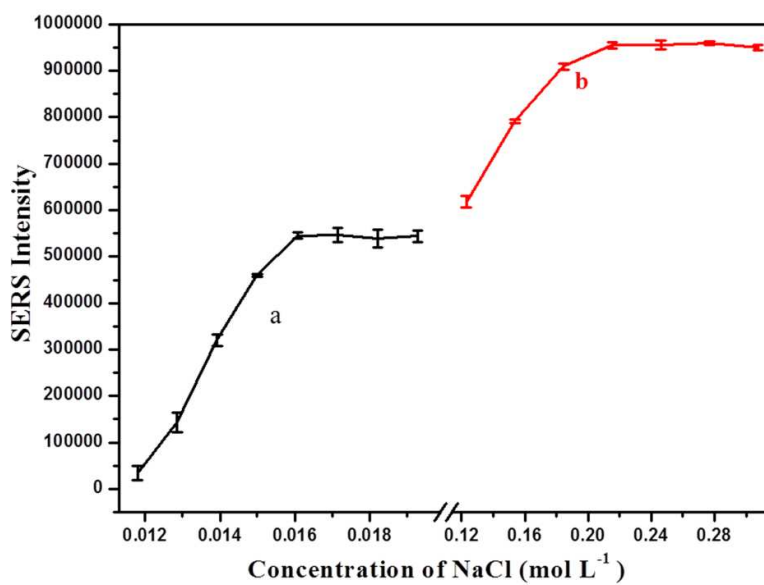


Fig. 6

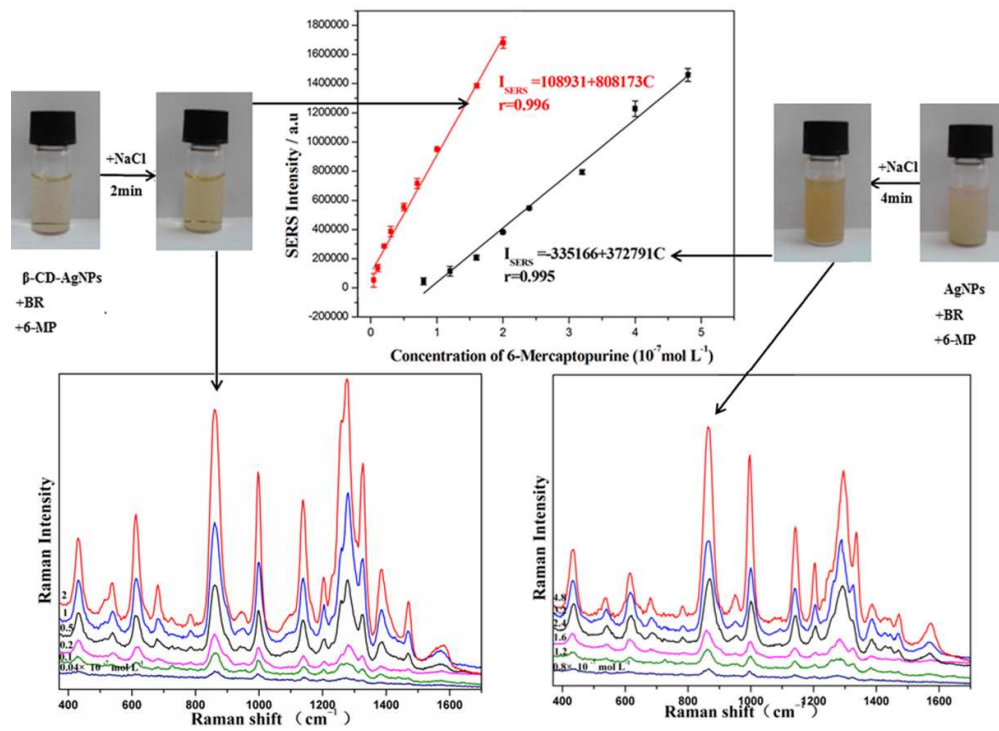


Fig. 7

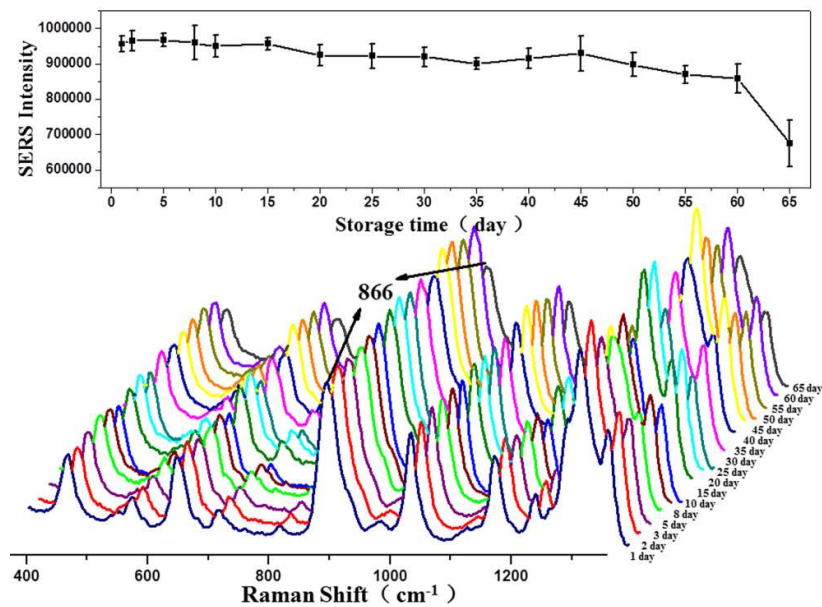


Fig. 8

**Table 1** Effect of coexisting substances

Coexisting substances	Concentration ( $\mu\text{mol}\cdot\text{L}^{-1}$ )	Relative error (%)	
		$\beta$ -CD-AgNPs	AgNPs
$\text{K}^+$ , $\text{Cl}^-$	200.0	-3.1	-6.5
$\text{Na}^+$ , $\text{Br}^-$	200.0	-5.4	-8.7
$\text{Co}^{2+}$ , $\text{Cl}^-$	200.0	-3.7	6.5
$\text{Fe}^{3+}$ , $\text{Cl}^-$	200.0	-1.5	3.1
$\text{Na}^+$ , $\text{HPO}_4^{2-}$	100.0	-2.3	-4.4
$\text{Mg}^{2+}$ , $\text{Cl}^-$	100.0	-1.7	2.6
$\text{Ca}^{2+}$ , $\text{Cl}^-$	100.0	1.2	-7.8
$\text{Na}^+$ , $\text{SO}_4^{2-}$	100.0	3.2	-4.3
$\text{Na}^+$ , $\text{CO}_3^{2-}$	100.0	-2.3	-8.6
$\text{Fe}^{2+}$ , $\text{Cl}^-$	100.0	-2.4	6.3
$\text{Cr}^{3+}$ , $\text{SO}_4^{2-}$	2.0	-0.7	-2.6
$\text{Ag}^+$ , $\text{NO}_3^-$	2.0	-1.5	-3.2
$\text{Ba}^{2+}$ , $\text{Cl}^-$	1.0	0.8	4.4
$\text{Hg}^{2+}$ , $\text{Cl}^-$	1.0	1.7	6.3
$\text{Ni}^+$ , $\text{Cl}^-$	1.0	-5.4	-13.3
$\text{Cu}^{2+}$ , $\text{Cl}^-$	1.0	3.1	9.4

**Table 2** Comparison of reported methods with the present method for the determination of 6-MP

Method	LOD ( $10^{-7}$ mol·L <sup>-1</sup> )	Linear range ( $10^{-7}$ mol·L <sup>-1</sup> )	References
SERS	0.024	0.040-2.0	This work
HPLC	0.20	0.10-6.4	19
Voltammetry	1.0	5.0-9000	23
The Desorption of Electrochemical Reduction	0.10	0.10-1.0	24
Electrochemistry	0.050	2.0-2000	25
Fluorescence Enhancement Method	0.0050	0.64-3.0	29

**Table 3** Recovery of 6MP detection in pharmaceutical tablets.

Sample	Silver nanoparticles	Added ( $10^{-7}$ mol·L <sup>-1</sup> )	Found ( $10^{-7}$ mol·L <sup>-1</sup> )	Recovery (%)	RSD (n=5, %)
Tablet 1	β-CD-AgNPs	1.00	1.03	103.0	2.45
	AgNPs	2.00	1.72	86.0	3.81
Tablet 2	β-CD-AgNPs	1.00	1.02	102.0	3.72
	AgNPs	2.00	1.53	76.5	4.19

1  
2  
3  
4 A high sensitive and selective method using silver nanoparticles decorated with  
5  
6  $\beta$ -cyclodextrinas SERS-active substrate was developed for detecting  
7  
8  
9 6-mercaptopurine.

